7
Duality

7.1 Introduction

For low energy scattering in the s channel it is often convenient to write the scattering amplitude as a partial-wave series (4.4.9)

$$A_{H_s}(s,t) = 16\pi \sum_J (2J+1)\, A_{HJ}(s)\, d^J_{\mu\mu'}(z_s) \tag{7.1.1}$$

because, as we have discussed in section 2.2, if the forces are of finite range, R, then for a given s only partial waves $J \lesssim (\sqrt{s})R/\hbar$ will be important. Furthermore the various partial-wave amplitudes are frequently dominated by resonance pole contributions, so, using the Breit–Wigner formula (2.2.15), we can write

$$A_{HJ}(s) \approx \sum_r \frac{g_r}{s_r - s}, \quad s_r \equiv M_r^2 - \mathrm{i}M_r\Gamma_r \tag{7.1.2}$$

and (7.1.2) in (7.1.1) often gives quite a good approximation to the low-energy scattering amplitude, for $s < 6\,\mathrm{GeV}^2$ say.

But as s increases the number of partial waves which must be included increases, and the density of resonances in each partial wave also seems to increase, so that it becomes harder to identify the individual resonance contributions. Hence (7.1.1) is much less useful for larger s. Also we know that it is not valid much beyond the s-channel physical region because the series diverges at the nearest t-singularity (at the boundary of the Lehmann ellipse (2.4.11)), so approximations to the scattering amplitude based on (7.1.1) are effective only in the region of the Mandelstam plot where s and $|t|$ are small, in the neighbourhood of the s-channel physical region (see fig. 1.5).

At high s on the other hand we have found it very useful to work instead with the t-channel partial-wave series, transformed via the Sommerfeld–Watson representation (4.6.4) into a sum of t-channel Regge poles and cuts. At high energies, say $s > 10\,\mathrm{GeV}^2$, only a few leading J-plane singularities need be included, but in principle this Sommerfeld–Watson representation is valid for all s and t.

The question thus arises as to how these two different viewpoints are to be married. This is an important practical problem in the inter-

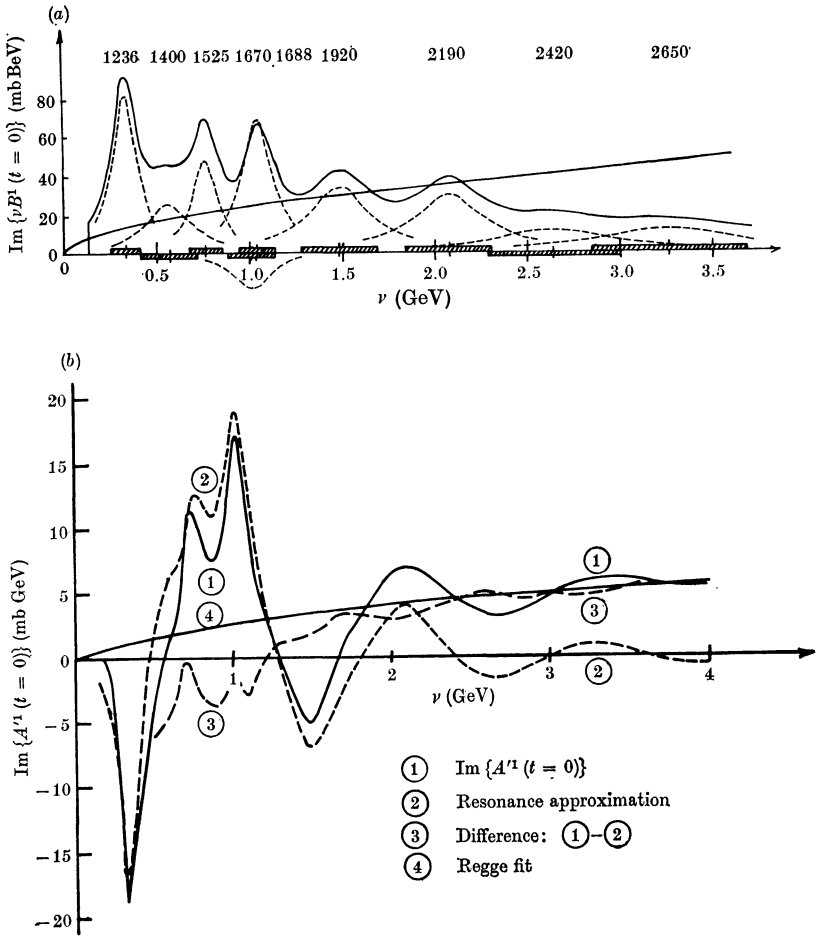

FIG. 7.1 The resonance and Regge pole contributions to (*a*) Im $\{\nu B\}$ and (*b*) Im $\{A'\}$ for $I_t = 1$ in $\pi^- p \to \pi^0 n$ at $t = 0$, from Dolen *et al.* (1968). At least at low energies the resonances almost saturate the amplitudes, while the ρ-pole Regge fit averages through the data. (For definition of ν see (7.2.3) below.)

mediate energy region, say $4 < s < 10\,\text{GeV}^2$, where the amplitudes are approaching their smooth Regge asymptotic s behaviour but some resonance bumps can still be seen (see fig. 7.1). It also poses a very important theoretical question as to how the s-channel resonances contribute to the asymptotic s behaviour, or, equivalently, where these resonances appear in the Sommerfeld–Watson representation.

Since all the residues g_r in (7.1.2) are constants, if there are only a finite number of resonances (however large), then clearly the total

https://doi.org/10.1017/9781009403269.008 Published online by Cambridge University Press

resonance contribution to the scattering amplitude must have the behaviour

$$A_H^{\mathrm{r}}(s,t) \sim \frac{1}{s}, \quad \text{for all fixed } t \tag{7.1.3}$$

and so would appear as a fixed pole at $J_t = -1$ in the Sommerfeld–Watson representation (from (2.7.2)). In this case one might try adding (7.1.2) and (4.6.4) giving

$$A_H(s,t) = A_H^{\mathrm{r}}(s,t) + A_H^{\mathrm{R}}(s,t) \tag{7.1.4}$$

where A^{r} includes all the s-channel resonances, and A^{R} all the t-channel Regge singularities with $\mathrm{Re}\{\alpha(t)\} > -1$. This is often called the interference model because the amplitude oscillates as a function of s because of interference between the resonances and the Regge poles (see for example Barger and Cline (1966, 1967)).

However, we have seen in chapter 3 how, in simple dynamical models like the ladder model, fig. 3.3, if the s-channel poles behave like s^{-1} then the t-channel trajectories obtain the asymptotic behaviour $\alpha(t) \xrightarrow[t \to -\infty]{} -1$ from above, from the unitarization of this fixed-pole input. And we have also found (fig. 6.6) that trajectories appear in practice to be essentially linear, $\alpha(t) \approx \alpha^0 + \alpha' t$, and seem to be descending well below -1. This could mean that somehow the fixed pole does not contribute to the leading Regge trajectories, but is to be added to them as in (7.1.4). For even-signature amplitudes, where $J = -1$ is a wrong-signature nonsense point, such an additional fixed pole is certainly possible (see sections 4.8 and 6.3), but in an odd-signature amplitude the fixed pole would be incompatible with t-channel unitarity. And a moving pole which remained in the region of $J_t = -1$ should have been observed by now in effective trajectory plots.

It seems fairly clear therefore that at least at large $-t$ the s-channel resonance poles are cancelling against each other in such a way as to produce an asymptotic behaviour $\sim s^x$, where $x \leqslant \alpha(t)$, $\alpha(t)$ being the leading t-channel singularity. The most interesting possibility is $x = \alpha(t)$, so that the s-channel resonances actually combine to produce the leading Regge pole behaviour. Of course this is only possible in the t region where $\alpha(t) > -1$ if there is an infinite number of resonances so that the series (7.1.2) diverges.

This possibility was first suggested in the now classic paper of Dolen, Horn and Schmid (1968), who noted that if one adds the contributions of all the resonances discovered by phase-shift analysts in πN scatter-

https://doi.org/10.1017/9781009403269.008 Published online by Cambridge University Press

ing (for $I_t = 1$) the result not only gives almost the whole scattering amplitude but is, on the average, approximately equal to the ρ-pole exchange contribution obtained from fits to high energy data, extrapolated down to the low-s region (see fig. 7.1). There thus seems to be an equivalence, an 'average duality', between the direct channel resonances, r, and the crossed channel Regge poles, R, because, at least in the intermediate energy region, the average of the former is equal to the latter, i.e.

$$\langle A_H(s,t)\rangle \approx \langle A_H^{\mathrm{r}}(s,t)\rangle \approx \langle A_H^{\mathrm{R}}(s,t)\rangle \tag{7.1.5}$$

(this statement is made more precise in the next section). One may then hope that as s is increased the density of resonances will also increase, thus smoothing out the bumps, until eventually there is 'local duality', i.e.

$$A_H(s,t) \approx A^{\mathrm{r}}(s,t) \approx A^{\mathrm{R}}(s,t) \tag{7.1.6}$$

without any need for averaging.

Unfortunately this argument is not completely compelling for at least two reasons. First, it is always possible to re-parameterize the Regge pole terms so as to retain their asymptotic behaviour but reduce their magnitude in the intermediate energy region. For example replacing $\beta(t)\,(s/s_0)^{\alpha(t)}$ by $\beta(t)\,[(s-s_a)/s_0)]^{\alpha(t)}$ reduces the magnitude in the neighbourhood of the arbitrarily chosen point s_a. Of course the branch point at $s = s_a$ would be spurious, but so is the one at $s = 0$ in the usual parameterization, which stems from the approximation (6.2.26). Essentially these two parameterizations differ just by terms of order $s^{\alpha(t)-1}$, i.e. at the daughter level, where the predictions of Regge theory are ambiguous.

Secondly, the actual identification of inelastic resonances in phase-shift analyses is called into question by the success of (7.1.5). For as Schmid (1968) showed, if one takes a Regge pole term (6.8.1), with a linear trajectory $\alpha(t) = \alpha^0 + \alpha' t$, and uses equal-mass kinematics (1.7.22)

$$z_s = 1 + \frac{t}{2q_s^2}, \quad q_s^2 = \frac{s-4m^2}{4},$$

the s-channel partial-wave projection (2.2.1) of the Regge term depends on (Chiu and Kotanski 1968)

$$A_J(s) \propto \int_{-1}^{1} \mathrm{e}^{-\mathrm{i}\pi\alpha(t)} P_J(z_s)\,\mathrm{d}z_s = \mathrm{e}^{-\mathrm{i}\pi(\alpha^0 - 2q_s^2\alpha')}(\mathrm{i})^J J_J(-2q_s^2\pi\alpha') \tag{7.1.7}$$

where J_J is the spherical Bessel function of order J (see for example

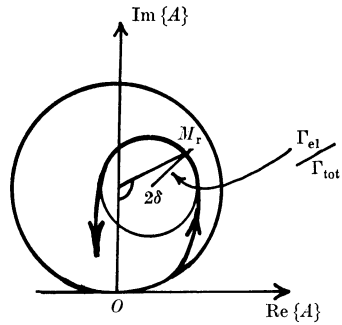

FIG. 7.2 The partial-wave Argand diagram for an inelastic resonance (see (2.2.13) *et seq.*). For a range of energies near M_r the curve follows a circle due to the Breit–Wigner formula, but it is smaller than the unitarity circle due to the inelasticity, and it is pushed off centre, and the phase may be rotated by the background.

Magnus and Oberhettinger (1949) p. 26). So as s (and hence q_s^2) increases the phase of the amplitude given by (7.1.7) will rotate anticlockwise, giving a loop just like that predicted for an inelastic resonance by (2.2.15) (see fig. 7.2). Note that if the phase reaches $\pi/2$ at a given 'resonance' position $s = s_r$, there will be further resonances at $s_r^n = s_r + n/\alpha'$, $n = 1, 2, \ldots$ where the phase goes through $(2n+1)\pi/2$, and all the partial waves will resonate at the same s_r^n since the phase in (7.1.7) is independent of J. Thus the Regge pole terms will give rise to resonance-like loops in the partial-wave Argand plots, despite the fact that the Regge pole term does not contain any poles in s.

There are clearly two ways of interpreting this result (Collins *et al.* 1968*b*). Either one accepts the postulate of duality, in which case these loops do correspond to resonances and are a manifestation of the average equality (7.1.5) even though the Regge terms do not contain s-channel poles. Or, if one chooses to deny duality, Argand loops can no longer be regarded as sufficient evidence for the existence of resonances, and there may well be fewer actual resonances than one has been led to suppose from phase-shift analyses. If so the phenomenological case for duality crumbles. The essence of this difficulty is that there can only be experimental evidence about the behaviour of scattering amplitudes along the real s axis, and so to analytically continue to the pole on the unphysical sheet requires a model based on unitarity. The Breit–Wigner formula (2.2.14) is certainly a valid model for elastic amplitudes dominated by isolated poles, but its use

for highly inelastic, overlapping groups of resonances is much more questionable; see Blatt and Weisskopf (1952), Weidenmuller (1967).

We shall put these doubts aside until the end of the chapter, where we shall be in a better position to review the quite strong evidence that the duality hypothesis is at least approximately valid. Our next step is to try and make the hypothesis a bit more precise.

7.2 Finite-energy sum rules

Finite-energy sum rules (FESR) are similar to the SCR of section 4.8, but apply also in circumstances where the amplitude is not convergent at infinity. All that is necessary is that the asymptotic behaviour be known. We shall assume for simplicity that the asymptotic behaviour is Regge-pole-like, so that, from (6.8.1)

$$\hat{A}_{H_t}(s,t) \xrightarrow[s\to\infty]{} \hat{A}^{\mathrm{R}}(s,t) = \sum_i -G_i(t)\frac{\mathrm{e}^{-\mathrm{i}\pi(\alpha-v)}+\mathscr{S}_i}{\sin\pi(\alpha-v)}\left(\frac{\nu}{s_0}\right)^{\alpha_i(t)-M} \tag{7.2.1}$$

where the sum is over all the leading Regge poles, say those with

$$\mathrm{Re}\{\alpha_i(t)\} > -k, \quad k > 1 \tag{7.2.2}$$

We have combined all the various residue factors into $G_i(t)$, and have introduced the notation

$$\nu \equiv \frac{s-u}{2} \tag{7.2.3}$$

So asymptotically

$$\left.\begin{aligned} D_s(s,t) &\xrightarrow[s\to\infty]{} \sum_i G_i(t)\left(\frac{\nu}{s_0}\right)^{\alpha_i(t)-M} \\ D_u(s,t) &\xrightarrow[s\to-\infty]{} \sum_i -\mathscr{S}_i G_i(t)\left(\frac{\nu}{s_0}\right)^{\alpha_i(t)-M}(-1)^{M-v} \end{aligned}\right\} \tag{7.2.4}$$

The scattering amplitude is expected to obey the fixed-t dispersion relation (4.5.1), and hence

$$\begin{aligned} \hat{A}_{H_t}(\nu,t) - \hat{A}^{\mathrm{R}}(\nu,t) = \frac{1}{\pi}\int_{\nu_{\mathrm{T}}}^{\infty} \frac{D_s(\nu',t) - \sum_i G_i(t)\,(\nu'/s_0)^{\alpha_i(t)-M}}{\nu'-\nu}\,\mathrm{d}\nu' \\ + \frac{1}{\pi}\int_{\nu_{\mathrm{T}}}^{\infty} \frac{D_u(\nu',t) - (-1)^{M-v}\sum_i \mathscr{S}_i G_i(t)\,(\nu'/s_0)^{\alpha_i(t)-M}}{\nu'+\nu}\,\mathrm{d}\nu' \end{aligned} \tag{7.2.5}$$

where $\nu_{\mathrm{T}}\,(\equiv s_{\mathrm{T}} + \frac{1}{2}(t-\Sigma))$ is the position of the s-threshold in terms of ν (where Σ is defined in (1.7.18)), and the integrals will converge. Because of the hypothesis (7.2.2) that all the leading terms in the

https://doi.org/10.1017/9781009403269.008 Published online by Cambridge University Press

asymptotic behaviour of $\hat{A}$ are contained in $\hat{A}^{\mathrm{R}}$ we know that at most

$$\hat{A} - \hat{A}^{\mathrm{R}} \sim \frac{1}{\nu^k}, \quad \nu \to \infty \tag{7.2.6}$$

so that when we take $\nu \to \infty$ on the right-hand side of (7.2.5) the coefficient of the ν^{-1} term must vanish, i.e.

$$\int_{\nu_{\mathrm{T}}}^{\infty} \left\{ D_s(\nu', t) - D_u(\nu', t) - \sum_i [1 - \mathscr{S}_i(-1)^{M-v}] G_i(t) \left(\frac{\nu'}{s_0}\right)^{\alpha_i(t)-M} \right\} \mathrm{d}\nu' = 0 \tag{7.2.7}$$

Obviously among all the poles, i, only a sub-set, denoted by j, which have signature

$$\mathscr{S}_j = (-1)^{M-v+1} \tag{7.2.8}$$

will contribute to (7.2.7).

Since the poles give the asymptotic form of D_s and D_u the integrand will be negligible for $\nu' > N$, for some sufficiently large N, and so

$$\int_{\nu_{\mathrm{T}}}^{N} (D_s(\nu', t) - D_u(\nu', t)) \, \mathrm{d}\nu' = \int_{\nu_{\mathrm{T}}}^{N} \sum_i 2G_i(t) \left(\frac{\nu'}{s_0}\right)^{\alpha_j(t)-M} \mathrm{d}\nu' \tag{7.2.9}$$

The integral on the right-hand side is readily performed to give the FESR

$$\int_{\nu_{\mathrm{T}}}^{N} (D_s(\nu', t) - D_u(\nu', t)) \, \mathrm{d}\nu' = \sum_i \frac{2s_0 G_j(t)}{\alpha_j(t) - M + 1} \times \left[\left(\frac{N}{s_0}\right)^{\alpha_j(t)-M+1} - \left(\frac{\nu_{\mathrm{T}}}{s_0}\right)^{\alpha_j(t)-M+1} \right] \tag{7.2.10}$$

For $\alpha_j > -1 + M$ the threshold term on the right-hand side can obviously be neglected if $N \gg s_0$.

An alternative way of deriving (7.2.10) (and its generalizations below), more elegant but perhaps less instructive, is to use Cauchy's theorem to write

$$\int_C \hat{A}_H(\nu', t) \, \mathrm{d}\nu' = 0 \tag{7.2.11}$$

where C is a contour which excludes the threshold branch points, as shown in fig. 7.3. So closing the contour onto the branch cuts gives

$$2\mathrm{i} \int_{\nu_{\mathrm{T}}}^{N} (D_s(\nu, t) - D_u(\nu', t)) \, \mathrm{d}\nu' = -\int_{C'} \hat{A}_{H_t}(\nu', t) \, \mathrm{d}\nu' \tag{7.2.12}$$

where C' is the circle at $|\nu| = N$. Putting $\nu = N \mathrm{e}^{\mathrm{i}\phi}$, replacing $\hat{A}_H$ by $\hat{A}_H^{\mathrm{R}}$ of (7.2.1), and taking proper care of the discontinuity of the Regge term across the branch cuts gives (7.2.10) without the threshold term.

The FESR (7.2.10) provides a relation between the average (i.e. the zeroth moment) of the imaginary part of the scattering amplitude at

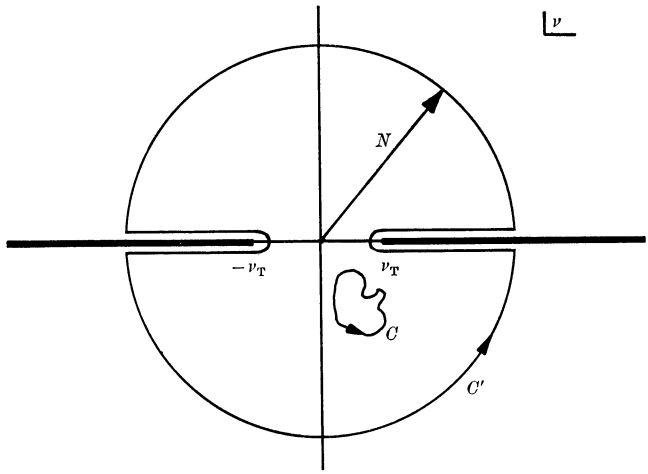

FIG. 7.3 Contours of integration in the complex ν plane for (7.2.11) and (7.2.12).

low energies and the Regge pole asymptotic behaviour at high energies, a relation which obtains because of the assumed analyticity of the amplitude and Regge pole dominance for $\nu \geqslant N$. This should clearly be helpful for understanding duality.

Several generalizations of (7.2.10) are possible. First, instead of (7.2.5) we can write the dispersion relation for

$$(\hat{A}_H(\nu,t)-\hat{A}_H^{\mathrm{R}}(\nu,t))\left(\frac{\nu}{s_0}\right)^{2n}, \quad n=0,1,2,\ldots \tag{7.2.13}$$

and as long as $2n < k$ the coefficient of the ν^{-1} term must vanish giving

$$\int_{\nu_T}^{N}(D_s(\nu',t)-D_u(\nu',t))\left(\frac{\nu'}{s_0}\right)^{2n}\mathrm{d}\nu' = \sum_j \frac{2s_0 G_j(t)}{\alpha_j(t)-M+2n+1} \times\left[\left(\frac{N}{s_0}\right)^{\alpha_j(t)-M+2n+1}-\left(\frac{\nu_T}{s_0}\right)^{\alpha_j(t)-M+2n+1}\right] \tag{7.2.14}$$

i.e. even-moment FESR. Alternatively, if an odd power of (ν/s_0) is included, only poles k with opposite signature to (7.2.8), i.e.

$$\mathscr{S}_k = (-1)^{M-v} \tag{7.2.15}$$

contribute, giving the odd-moment FESR

$$\int_{\nu_T}^{N}(D_s(\nu',t)+D_u(\nu't))\left(\frac{\nu'}{s_0}\right)^{2n-1}\mathrm{d}\nu' = \sum_k \frac{2s_0 G_k(t)}{\alpha_k(t)-M+2n} \times\left[\left(\frac{N}{s_0}\right)^{\alpha_k(t)-M+2n}-\left(\frac{\nu_T}{s_0}\right)^{\alpha_k(t)-M+2n}\right] \tag{7.2.16}$$

https://doi.org/10.1017/9781009403269.008 Published online by Cambridge University Press

(the + sign appearing on the left-hand side because of the odd power of ν). These integrals involve only the imaginary part of the scattering amplitude, but it is possible to include both real and imaginary parts by writing a dispersion relation for (Liu and Okubo 1967)

$$(\hat{A}_H(\nu,t)-\hat{A}_H^{\mathrm{R}}(\nu,t))\left(\frac{\nu_{\mathrm{T}}^2-\nu^2}{s_0^2}\right)^{\beta/2} \tag{7.2.17}$$

where β is an arbitrary parameter, giving

$$\int_{\nu_{\mathrm{T}}}^{N}\left[\cos\left(\frac{\pi\beta}{2}\right)\mathrm{Im}\{\hat{A}_{H_t}(\nu',t)\}-\sin\left(\frac{\pi\beta}{2}\right)\mathrm{Re}\{\hat{A}_{H_t}(\nu',t)\}\right]\left(\frac{\nu'^2-\nu_{\mathrm{T}}^2}{s_0^2}\right)^{\beta/2}\mathrm{d}\nu'$$

$$=\sum_i\frac{2s_0G_i(t)}{\alpha_i(t)+\beta+1}\left(\frac{N}{s_0}\right)^{\alpha_i(t)+\beta+1}\frac{\cos[\frac{1}{2}\pi(\alpha_i(t)+\beta)]}{\cos(\frac{1}{2}\pi\alpha_i(t))} \tag{7.2.18}$$

which for example reduces to (7.2.14) (without the ν_{T} term) for $\beta=$ even integer. These are called continuous moment sum rules (CMSR), but as information about the real parts of amplitudes is seldom available except from dispersion relations which have clearly been assumed in deriving (7.2.18) CMSR are only occasionally useful.

It is also interesting to write FESR for amplitudes of definite signature which have the fixed-t dispersion relations (like (2.5.7))

$$\hat{A}_H^{\mathscr{S}}(s,t)=\frac{1}{\pi}\int_{s_{\mathrm{T}}}^{\infty}\frac{D_s(s',t)}{s'-s}\,\mathrm{d}s'+(-1)^{M-v}\mathscr{S}\int_{u_{\mathrm{T}}}^{\infty}\frac{D_u(s',t)}{s'-s}\,\mathrm{d}s' \tag{7.2.19}$$

so if we follow the above procedure we find

$$\int_{\nu_{\mathrm{T}}}^{N}[D_s(\nu',t)+(-1)^{M-v}D_u(\nu',t)]\left(\frac{\nu'}{s_0}\right)^n\mathrm{d}\nu'$$

$$=\sum_l\frac{2s_0G_l(t)}{\alpha_l(t)-M+n+1}\left(\frac{N}{s_0}\right)^{\alpha_l(t)-M+n+1},\quad n=0,1,2,\ldots \tag{7.2.20}$$

where $l=j$ or k depending on $\mathscr{S}$ (see (7.2.8), (7.2.15)). These FESR coincide with (7.2.14) or (7.2.16) only for alternate moments. But the 'wrong moments' (i.e. n even for $\mathscr{S}=(-1)^{M-v}$ or n odd for $\mathscr{S}=(-1)^{M-v+1}$) are likely to be incorrect because we have neglected the fact that definite-signature amplitudes contain fixed poles at wrong-signature nonsense points (see section 4.8) which should also be included in the right-hand side of (7.2.20). So for wrong moments we must add

$$\sum_l\frac{G_l(t)}{J_l-M+n+1}\left(\frac{N}{s_0}\right)^{J_l-M+n+1} \tag{7.2.21}$$

to the right-hand side of (7.2.20), where J_l are the positions of the wrong-signature nonsense fixed poles, i.e. $J_l=M-1,M-3,\ldots$ or

https://doi.org/10.1017/9781009403269.008 Published online by Cambridge University Press

$M-2, M-4, \ldots$ for $\mathscr{S} = \pm(-1)^{M-v}$. However, if the fixed-pole residues are small (7.2.20) will be approximately valid as it stands for all moments.

We shall discuss some of the phenomenological applications of FESR in the next section, but here our main interest is to examine the implications of duality for FESR. If the imaginary part of the scattering amplitude at low energy can be represented as a sum of resonance pole contributions (r), (7.2.10) becomes

$$\int_{\nu_T}^{N} [D_s^r(\nu', t) - D_u^r(\nu', t)] \, d\nu' = \sum_j \frac{2s_0 G_j(t)}{\alpha_j(t) - M + 1} \left(\frac{N}{s_0}\right)^{\alpha_j(t) \quad M+1} \tag{7.2.22}$$

This gives a definite meaning to (7.1.5), that the integral of the imaginary part of the resonance contributions to the scattering amplitude is equal to that of the Regge pole contributions (fig. 7.1). Note, however, that to obtain (7.2.22) we have already made the duality assumption because the sum of a finite set of resonances $\sim s^{-1}$, but in (7.2.2) we assumed that the Regge poles include all the leading terms in asymptotic behaviour down to s^{-k}, $k > 1$. So (7.2.22) does not in any sense prove duality, but it does give it a more concrete mathematical expression than (7.1.5).

The higher-moment sum rules require a more local duality and so are less likely to work at low energies. If all the moments were the same then of course A^r would be identically equal to A^R, which is clearly impossible since the one contains poles in s and the other does not.

The constraints imposed on an amplitude by (7.2.22) are quite powerful if crossing is also incorporated. For example if we consider $\pi\pi$ scattering (Gross (1967); see also Collins and Mir (1970)), the dominant $I_t = 1$, odd-signature exchange will be the ρ trajectory (see section 3.5). However ρ poles with spin $\sigma = 1$ will also be the principal s- and u-channel resonances so (see (2.6.13))

$$\begin{aligned} D_s^r &= 16\pi^2 3 \frac{\beta(s)}{\alpha'} P_1(z_s) \delta(s - m_\rho^2) \\ &= 16\pi^2 3 \frac{\beta(s)}{\alpha'} \left(1 + \frac{2t}{m_\rho^2 - 4}\right) \delta(s - m_\rho^2) \end{aligned} \tag{7.2.23}$$

if we use units where $m_\pi = 1$. We take the residue to be

$$\beta(s) = \frac{\gamma(s)\,\alpha(s)}{\Gamma(\alpha + \frac{3}{2})} (q_s^2)^{\alpha(s)}, \quad \text{where} \quad \alpha(m_\rho^2) = 1, \quad q_s^2 = \frac{s-4}{4} \tag{7.2.24}$$

$\gamma(s)$ being the reduced residue, remaining after we have extracted explicitly the threshold behaviour (6.2.9), the nonsense factor at $\alpha = 0$, and the Mandelstam-symmetry zeros (2.9.5). This gives

$$D_s^{\mathrm{r}}(s,t) = 64(\pi)^{\frac{3}{2}} \frac{\gamma(m_\rho^2)}{\alpha'} \left(\frac{m_\rho^2 - 4}{4}\right) \left(1 + \frac{2t}{m_\rho^2 - 4}\right) \delta(s - m_\rho^2) \quad (7.2.25)$$

and likewise for $D_u^{\mathrm{r}}(s,t)$. Similarly the ρ trajectory in the t channel will give, using (6.8.1),

$$D_s^{\mathrm{R}}(s,t) = 16(\pi)^{\frac{3}{2}} \gamma(t) \frac{\alpha(t)}{\Gamma(\alpha+1)} \nu^{\alpha(t)} \quad (7.2.26)$$

Substituting (7.2.25) and (7.2.26) into (7.2.22) (remembering that we are considering an amplitude for spinless particles so $M = 0$, and with $I_t = 1$ so that the left-hand side must include a crossing matrix element $\frac{1}{2}$ from table 6.3 which cancels the factor 2 from adding D_s and D_u) we obtain

$$2 \frac{\gamma(m_\rho^2)}{\alpha'} \left(\frac{m_\rho^2 - 4}{4}\right) \left(1 + \frac{2t}{m_\rho^2 - 4}\right) = \frac{\gamma(t)\,\alpha(t)}{\Gamma(\alpha(t)+1)\,(\alpha(t)+1)} N^{\alpha(t)+1} \quad (7.2.27)$$

If these are equated at $t = m_\rho^2$ the γ's cancel out, $\alpha(t) = 1$, and we get

$$\alpha' = \frac{3m_\rho^2 - 4}{N^2}$$

So taking the cut-off, N, half way between the $\rho(m_\rho^2 \approx 30m_\pi^2)$ and the next s-channel resonance, the f $(m_f^2 \approx 80m_\pi^2)$, i.e. taking $N = 68m_\pi^2$ (from (7.2.3)), we get $\alpha' = 0.019 m_\pi^{-2} = 1\,\mathrm{GeV}^2$

in quite good agreement with (5.3.1). If we take the nth moment sum rule, and ignore the possibility of fixed poles, we get

$$\alpha' = \frac{n+2}{2^{n+1}} \frac{(3m_\rho^2 - 4)^{n+1}}{N^{n+2}}$$

which with $N = 68$ gives a rather slow variation of α' with n for small n, so all the low moments are quite well satisfied.

Equation (7.2.27) is an FESR consistency condition for the ρ trajectory, sometimes called an 'FESR bootstrap'. It is quite different from a proper bootstrap of the type discussed in section 3.5 (and section 11.7 below) because no attempt is made to impose unitarity, and hence the magnitude of the coupling, $\gamma(t)$, factors out. Also it is necessary to know the particle spectrum before one can fix N, so the

https://doi.org/10.1017/9781009403269.008 Published online by Cambridge University Press

trajectory is not determined uniquely. And we have chosen to evaluate the sum rule at $t = m_\rho^2$, but it is evident that the t-dependence of the two sides of (7.2.27) is quite different. None the less before the advent of more complete dual models (see section 7.4) a good deal of work went into showing that these consistency relations do apply quite widely (see for example Ademollo *et al.* (1958, 1969), Igi and Matsuda (1967)). Their SU(3) generalization will be discussed below.

7.3 Applications of FESR and duality

The first point to note about the duality hypothesis in the form (7.2.22) is that it is clearly invalid for Pomeron (P) exchange. For example both $pp \to pp$ and $K^+p \to K^+p$ elastic scattering amplitudes have exotic quantum numbers (see section (5.2)) and do not contain any s-channel resonances, but are controlled by the t-channel P exchange. This observation led to the hypothesis of 'two-component duality' (Harari 1968, Freund 1968) which states that where vacuum quantum numbers occur in the t channel the ordinary Reggeons, R (i.e. all except P) are dual to the resonances (r), while the P is dual to the background amplitude (b) upon which the resonances are superimposed. So such amplitudes have two components

$$A_H(s,t) = A^{\mathrm{r}}(s,t) + A^{\mathrm{b}}(s,t) = A^{\mathrm{R}}(s,t) + A^{\mathrm{P}}(s,t) \qquad (7.3.1)$$

with

$$\langle \mathrm{A}^{\mathrm{r}} \rangle = A^{\mathrm{R}} \quad \text{and} \quad \langle A^{\mathrm{b}} \rangle = A^{\mathrm{P}} \qquad (7.3.2)$$

the averages being taken for the imaginary parts in the sense of (7.2.22). Of course for processes where P exchange cannot occur (7.1.6) holds, and only one component is necessary.

This hypothesis has been tested directly in πN elastic scattering (e.g. Harari and Zarmi 1969) by showing that the sum of the resonances (represented by inelastic Breit–Wigner formulae) and the P amplitude (extrapolated from high-energy fits) can reproduce the scattering amplitudes obtained in low energy phase-shift analyses. Of course, as most of these resonances were actually discovered in phase-shift analyses, the test really amounts to showing (*a*) that the Breit–Wigner formula (2.2.15) without any rotation of phase parameterizes the resonance loops satisfactorily, and (*b*) that the extrapolated P amplitude can account for all the background to these resonances. Unfortunately this is not sufficient to prove the hypothesis because by giving the Breit–Wigner formulae arbitrary phases, which is not

unreasonable for highly inelastic overlapping sets of resonances, the interference model

$$A = A^{\mathrm{P}} + A^{\mathrm{R}} + A^{\mathrm{r}} \tag{7.3.3}$$

can be made to fit equally well (Donnachie and Kirsopp 1969), quite apart from the uncertainty which exists in the resonance interpretation of the phase shifts mentioned in section 7.1. But the fact that it is possible to construct consistent dual models, and apply (7.3.2) in a wide variety of situations (see also section 10.7) makes it seem likely that this two-component hypothesis has at least approximate validity.

Why the P should have this exceptional status is not completely clear. We shall discuss some plausible dynamical reasons in section 11.7, but we have already noted that the slope of the P is only $\alpha'_{\mathrm{P}} \approx 0.2\,\mathrm{GeV}^2$, compared with $\alpha'_{\mathrm{R}} \simeq 0.9\,\mathrm{GeV}^2$ for all the other trajectories, so that any resonance-like loops generated by the P in (7.1.7) would have a very slow phase rotation, and would be very widely spaced.

There still remains, however, the problem that exotic channels like $\mathrm{pp} \to \mathrm{pp}$ and $\mathrm{K^+p} \to \mathrm{K^+p}$ can exchange other trajectories, $R = \rho$, A_2 ω and f (table 6.5), despite the fact that they contain no resonances. This can be accounted for by invoking strong exchange degeneracy (section 6.8*h*), and supposing that as in (6.8.22) the contributions of these trajectories cancel, $A_2 - \rho$ and $\mathrm{f} - \omega$, leaving no imaginary part. This can occur if the signs of the different contributions are arranged as in table 7.1. Since Breit–Wigner resonances dominate $\mathrm{Im}\{A(s,t)\}$ (see (2.2.15)) the absence of an imaginary part to A^{R} implies, via (7.2.22) and (7.3.2), that there will be no resonances. Alternatively, resonances could occur with alternating signs to give $\langle \mathrm{Im}\ \{\mathrm{A^r}\}\rangle = 0$ averaged over several resonances, but clearly this is not the solution we want for exotic elastic processes.

It is thus essential that the degeneracy pattern of Regge exchanges should be consistent with the resonance spectrum. This explains the fact that the exotic processes have rather flat $\sigma^{\mathrm{tot}}(s)$, and only a simple exponential behaviour of $\mathrm{d}\sigma/\mathrm{d}t$ as a function of t from P exchange, while the non-exotic line-reversed processes $\bar{\mathrm{p}}\mathrm{p} \to \bar{\mathrm{p}}\mathrm{p}$ and $\mathrm{K^-p} \to \mathrm{K^-p}$, in which the sign of the odd signature ρ and ω exchanges is reversed, have falling $\sigma^{\mathrm{tot}}(s)$, and dip structures at low energy at $|t| \approx 0.55\,\mathrm{GeV}^2$ due to the R contribution (see for example figs. 6.4 and 6.5). We shall examine the implications of these exchange-degeneracy requirements more fully below.

FESR provide a new tool for Regge analysis, because if one knows

https://doi.org/10.1017/9781009403269.008 Published online by Cambridge University Press

Table 7.1 *Signs of the trajectory contributions to the imaginary part of the elastic* NN *and* KN *scattering amplitudes*

Process	Exchanges
$\bar{p}p \to \bar{p}p$	$P+f+\rho+\omega+A_2$
$\bar{p}n \to \bar{p}n$	$P+f-\rho+\omega-A_2$
$pp \to pp$	$P+f-\rho-\omega+A_2$
$pn \to pn$	$P+f+\rho-\omega-A_2$
$K^-p \to K^-p$	$P+f+\rho+\omega+A_2$
$K^-n \to K^-n$	$P+f-\rho+\omega-A_2$
$K^+p \to K^+p$	$P+f-\rho-\omega+A_2$
$K^+n \to K^+n$	$P+f+\rho-\omega-A_2$

Under $p \leftrightarrow n$ odd-isospin ρ and A_2 change sign. Under particle $\leftrightarrow$ anti-particle the odd-C_n ρ and ω change sign.

the low energy amplitude, from, for example, a phase-shift analysis, one can use (7.2.14) and (7.2.16) to determine the Regge parameters without recourse to high energy data. This was done by Dolen *et al.* (1968) who for example used the difference of the $\pi^{\pm}p \to \pi^{\pm}p$ elastic scattering amplitudes obtained from an $E < 1.5\,\text{GeV}$ phase-shift analysis to obtain the ρ-exchange parameters from (7.2.22) (see fig. 7.1).

Since even with a single trajectory exchange there are two parameters in (7.2.14) for each value of t, $\alpha(t)$ and $G(t)$, the sum rules do not have a unique solution. But if we define for the non-flip, $M = 0$ amplitude

$$S_m(t) = \frac{1}{N^{m+1}} \int_0^N \nu^m D_s^{\mathscr{S}}(\nu', t)\, \mathrm{d}\nu' = \frac{2G(t)\, N^{\alpha(t)}}{\alpha(t)+m+1} \qquad (7.3.4)$$

(using the notation of (7.2.4), and setting $s_0 = 1$) then the ratio

$$\frac{S_{m'}(t)}{S_m(t)} = \frac{\alpha(t)+m'+1}{\alpha(t)+m+1} \qquad (7.3.5)$$

so $\alpha(t)$ can be obtained from the ratio of the first two right-signature moments ($m = 0$ and $m = 2$ for the $\mathscr{S} = -1$ ρ), and then re-inserted in (7.3.4) to find $G(t)$. Their results were in good agreement with the ρ parameters obtained by fitting the high energy data.

The various resonance contributions have different t dependences, being proportional to $d^{\sigma}_{\mu\mu'}(z_s)$, where σ is the spin of the resonance. These rotation functions are oscillatory functions of z_s (and hence of t at fixed s) and so it is found that at some t values the left-hand side of (7.3.4) vanishes. This occurs for $\mathrm{Im}\{A_{++}(\nu, t)\}$ at $t \approx -0.15\,\text{GeV}^2$,

https://doi.org/10.1017/9781009403269.008 Published online by Cambridge University Press

where the cross-over zero appears in the Regge amplitude, and in $\mathrm{Im}\{A_{+-}(s,t)\}$ at $t \approx -0.55\,\mathrm{GeV}^2$, coincident with the nonsense zero (see sections 6.8*k*, *l*). To build up the Regge behaviour with the correct t dependence for the residues there has to be a very close correlation between the contributions of the various resonances.

Of course this use of FESR suffers from the same sort of ambiguity concerning secondary trajectories, cuts etc, as do the high energy fits, but at least in principle these secondary contributions may also be identified. Thus if there is a secondary ρ' trajectory, $\alpha_1(t)$, in addition to the ρ, we deduce from (7.3.4)

$$\frac{S_0(t) - G(t)\,N^{\alpha(t)}/(\alpha(t)+1)}{S_2(t) - G(t)\,N^{\alpha(t)}/(\alpha(t)+3)} = \frac{\alpha_1(t)+3}{\alpha_1(t)+1} \tag{7.3.6}$$

so once $\alpha(t)$, $G(t)$ have been found, it is possible to obtain $\alpha_1(t)$, and so on. In fact Dolen *et al.* obtained the very high secondary trajectory $\alpha_1(t) = 0.3 + 0.8t$, which probably mainly reflects the build-up of errors which occurs when parameters are determined successively like this.

The higher-moment sum rules weight the integrals more towards the upper limit of integration, and if N is sufficiently large use of FESR becomes essentially equivalent to making a Regge fit near N. But in practice N has to be quite low because phase-shift analyses do not extend far in energy ($< 3\,\mathrm{GeV}$). This means that the results obtained depend greatly on the assumptions which are made about the high energy behaviour, and in practice with data of finite accuracy it is not possible to predict a unique analytic extrapolation. So the predictive power of the method for determining the high energy behaviour of amplitudes from low energy data alone is very limited. Certainly it provides no substitute for high energy data. Also phase-shift analyses are available only for a few channels ($\pi N \to \pi N$, $KN \to KN$, $\gamma N \to \pi N$ and $\pi N \to \pi\Delta$ at present) so the number of processes to which the method can be applied directly, even after invoking isospin relations like (6.8.23), is somewhat limited. Quite often FESR can be employed in other processes by making extra assumptions such as resonance saturation of the low energy amplitude (which we used for the $\pi\pi$ amplitude in the previous section) though obviously the uncertainty of the results is increased thereby.

There is, however, one crucial advantage of the FESR method over conventional Regge fits, namely that the phase-shift analysis gives the input amplitudes A_{H_s} directly, whereas $\mathrm{d}\sigma/\mathrm{d}t$ data only give

https://doi.org/10.1017/9781009403269.008 Published online by Cambridge University Press

$\sum_{H_s} |A_{H_s}|^2$. Thus with FESR one can find the Regge behaviours of the different spin amplitudes separately, and determine their phases, without recourse to polarization or other spin-dependent measurements. Thus much of the information contained in the 6 GeV πN amplitude analysis discussed in section 6.8*m* could also be obtained, at least qualitatively, by extrapolating the < 2 GeV phase-shift solutions with FESR, assuming Regge behaviour.

So FESR, especially when used in conjunction with fits to high energy data, are a very valuable aid to Regge analysis (see Barger and Phillips (1969) for examples of their use).

7.4 The Veneziano model

Much of the progress which has been made in applying and generalizing the concept of duality stems from the success of Veneziano (1968) in constructing a simple model for $2 \to 2$ scattering amplitudes which satisfies most of the requirements of duality.

We begin by considering the amplitude for $\pi^+\pi^- \to \pi^+\pi^-$, which has ρ and f poles in the s and t channels, but for which the u-channel $\pi^+\pi^+ \to \pi^+\pi^+$ is exotic, $I_u = 2$. So once the P component has been removed from this elastic scattering process we expect the approximately degenerate ρ and f trajectories to give the leading contributions in both channels, but there may be an infinite number of other resonances with these same quantum numbers.

The duality requirement (7.3.2) is that the sum over all the s-channel poles should be equal to the sum over all the t-channel poles, i.e.

$$A(s,t) = \sum_n \frac{G_n(s,t))}{s - s_n} = \sum_m \frac{G_m(t,s)}{t - t_m} \tag{7.4.1}$$

and that Regge asymptotic behaviour occur in both variables, i.e.

$$A(s,t) \underset{s\to\infty}{\sim} s^{\alpha(t)} \quad (t \text{ fixed}), \quad \text{and} \quad A(s,t) \underset{t\to\infty}{\sim} t^{\alpha(s)} \quad (s \text{ fixed}) \tag{7.4.2}$$

The simplest function which has an infinite set of s-poles lying on a trajectory $\alpha(s)$, the poles occurring when $\alpha(s) =$ positive integer, is $\Gamma(1-\alpha(s))$. Since we need an identical behaviour in t as well we might try

$$A(s,t) = \Gamma(1-\alpha(s))\,\Gamma(1-\alpha(t)) \tag{7.4.3}$$

but this would give a double pole at each s–t point where both $\alpha(s)$ and $\alpha(t)$ are positive integers (see fig. 6.4). However, these double poles can

https://doi.org/10.1017/9781009403269.008 Published online by Cambridge University Press

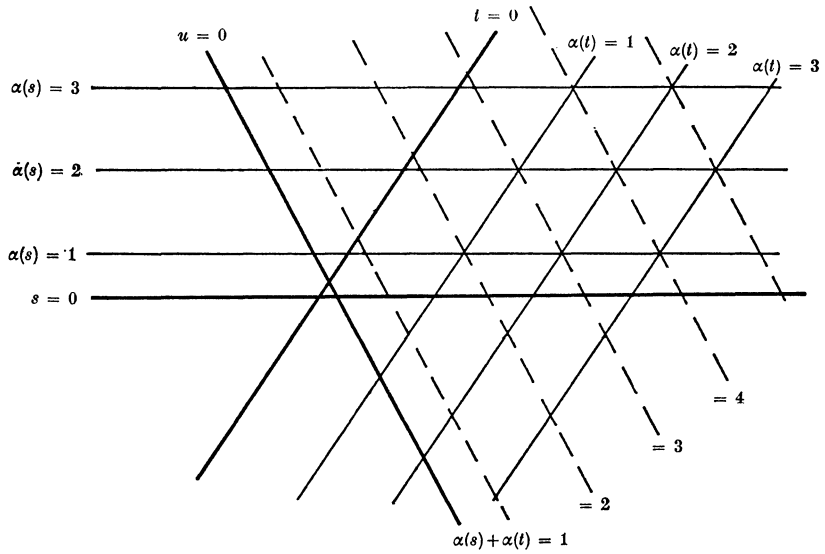

FIG. 7.4 Poles of the Veneziano amplitude in the s–t plane. The poles occur where $\alpha(s)$ and $\alpha(t)$ pass through positive integers, with lines of zeros connecting the pole intersections to prevent double poles.

easily be removed by writing

$$A(s,t) = V(s,t) \equiv g\,\frac{\Gamma(1-\alpha(s))\,\Gamma(1-\alpha(t))}{\Gamma(1-\alpha(s)-\alpha(t))} \tag{7.4.4}$$

which is the Veneziano formula. Here g is an arbitrary number which sets the scale of the coupling strengths as we shall see below (equation (7.4.12)).

The asymptotic behaviour of this amplitude may be deduced from Stirling's formula (see for example Magnus and Oberhettinger (1949) p. 4)

$$\Gamma(x) \underset{x\to\infty}{\longrightarrow} (2\pi)^{\frac{1}{2}}\,\mathrm{e}^{-x}\,x^{x-\frac{1}{2}} \tag{7.4.5}$$

(except in a wedge along the real negative x axis where poles appear for integer x) which gives

$$\frac{\Gamma(x+a)}{\Gamma(x+b)} \underset{x\to\infty}{\longrightarrow} x^{a-b}\left(1+O\left(\frac{1}{x}\right)\right) \tag{7.4.6}$$

Hence if $\alpha(s)$ is an increasing function of s we have, for fixed t (using (6.2.32)),

$$V(s,t) \underset{s\to\infty}{\longrightarrow} g\,\frac{\pi(-\alpha(s))^{\alpha(t)}}{\Gamma(\alpha(t))\sin\pi\alpha(t)} \tag{7.4.7}$$

https://doi.org/10.1017/9781009403269.008 Published online by Cambridge University Press

Then if $\alpha(s)$ is a linear function, $\alpha(s) \underset{s\to\infty}{\to} \alpha^0 + \alpha' s$, we get

$$V(s,t) \xrightarrow[s\to\infty]{} g \frac{\pi(-\alpha' s)^{\alpha(t)}}{\Gamma(\alpha(t)) \sin \pi\alpha(t)} = g \frac{\pi(\alpha' s)^{\alpha(t)}}{\Gamma(\alpha(t)) \sin \pi\alpha(t)} e^{-i\pi\alpha(t)} \quad (7.4.8)$$

which gives the required Regge behaviour (but not for real positive s). And since (7.4.4) is symmetrical in s and t, the corresponding result obviously holds for $t \to \infty$ at fixed s.

The formula (7.4.4) has several notable properties: (*a*) It is manifestly crossing symmetric, and so has the same poles and Regge behaviour in both s and t. (*b*) To get the required Regge behaviour we have had to demand that the trajectory be asymptotically linear, which is quite compatible with the observed linear behaviour for small $|s|$, which has puzzled us hitherto. (*c*) It has poles for positive integer $\alpha(t)$ only, since the nonsense factor $[\Gamma(\alpha(t))]^{-1}$ removes the poles for $\alpha(t) \leqslant 0$. (*d*) It has the rotating phase (6.8.21) expected from the sum of two exchange-degenerate trajectories. This ensures that, for $s > 0$, $\mathrm{Im}\{V(s,t)\} \sim s^{\alpha(t)}$, but for $s < 0$, in the u-channel physical region $\mathrm{Im}\{V(s,t)\} = 0$, since the u-channel is exotic. However, since the poles are on the real axis the discontinuity in either the s or t channels is just a sum of δ functions, and the double spectral function is the mesh of points where the poles cross in fig. 7.4. (*e*) The scale factor in the asymptotic behaviour (7.4.8) is given by

$$s_0 = \alpha'^{-1} \quad (7.4.9)$$

and we have already noted that empirically $s_0 \approx 1\,\mathrm{GeV}^2$ and $\alpha' \approx 1\,\mathrm{GeV}^{-2}$.

To obtain the resonance spectrum in the s channel we use the result (Magnus and Oberhettinger (1949) p. 2)

$$\frac{\Gamma(x)\Gamma(a+1)}{\Gamma(x+a)} = \sum_{n=0}^{\infty} (-1)^n \frac{\Gamma(a+1)}{\Gamma(a-n)\Gamma(n+1)} \cdot \frac{1}{x+n}, \quad a \text{ real} > 0 \quad (7.4.10)$$

to write

$$V(s,t) = \sum_{n=1}^{\infty} g \frac{\Gamma(1-\alpha(t))}{\Gamma(n)\Gamma(1-n-\alpha(t))} \frac{(-1)^n}{\alpha(s)-n} \quad (7.4.11)$$

so that if $\alpha(s) \to n$ for $s \to s_n$ (say) there is a pole of the form

$$V(s,t) \xrightarrow[s\to s_n]{} g \frac{(n-\alpha(t)-1)(n-\alpha(t)-2)\ldots(-\alpha(t))}{(n-1)!\,\alpha'(s-s_n)} \quad (7.4.12)$$

So if $\alpha(t) = \alpha^0 + \alpha' t$ the residue of the pole is a polynomial in $t\,[= -2q_s^2(1-z_s)]$ of order n, and

$$V(s,t) \xrightarrow[s\to s_n]{} \frac{g}{\alpha'(s-s_n)(n-1)!} [(2q_s^2\alpha' z_s)^n + O(z_s^{n-1})] \quad (7.4.13)$$

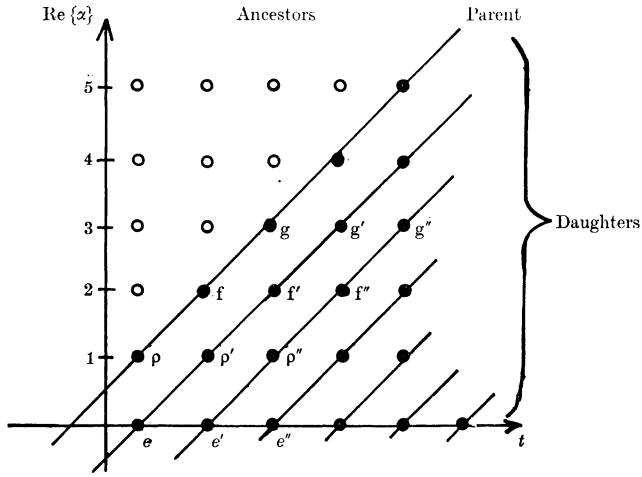

FIG. 7.5 The ε, ρ, f, g, ... states required in the Veneziano model for ππ scattering. The open circles are positions where ancestors occur if complex α's are used.

and hence the residue may be rewritten as a sum of Legendre polynomials, $P_n(z_s)$, $P_{n-1}(z_s)$, ..., $P_0(z_s)$. Thus the pole at $s = s_n$ corresponds to a degenerate sequence of $n+1$ resonances having spins $= 0, 1, \ldots, n$. The resulting resonance spectrum, an infinite sequence of integrally spaced daughters, is shown in fig. 7.5 where we have given particle names to the lowest mass states.

Since the Veneziano model is an analytic function of s and t, with just poles, and has the correct asymptotic behaviour, it clearly should provide a solution to the FESR consistency condition (7.2.22). This is not quite trivial because the Regge asymptotic behaviour does not hold along the real positive s axis. The relation between the residues in the two channels, each being proportional to g, is reminiscent of our approximate solution (7.2.27). A fairly complete review of the properties of the Veneziano formula and FESR tests can be found in Sivers and Yellin (1971).

The most obvious defect of the Veneziano model is that the poles appear on the real s axis, and so we do not get Regge behaviour where it is actually seen experimentally. This is because we have used real trajectory functions, whereas we know from section 3.2 that above the threshold in each channel unitarity requires that trajectories become complex (Im $\{\alpha\}$ being proportional to Γ, the width of the resonance – see (2.8.7)), and the poles move off the physical sheet.

It seems rather obvious therefore that one should insert complex

https://doi.org/10.1017/9781009403269.008 Published online by Cambridge University Press

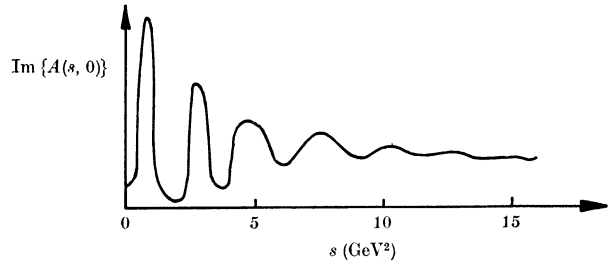

FIG. 7.6 The imaginary part of the amplitude for a Veneziano model for $\pi\pi$ scattering with complex α's.

trajectories satisfying dispersion relations like (3.2.12) into (7.4.4). However, if we do so the residues of the poles at $s = s_n$ in (7.4.12) cease to be polynomials in t, so that (7.4.13) is no longer applicable, and each pole gives rise to resonances of arbitrarily high spin. We should thus produce the so-called 'ancestor' poles of fig. 7.5. Despite the occurrence of these ancestors the asymptotic behaviour is still (7.4.8) which shows that the amplitude no longer has the convergent large-l behaviour needed for Carlson's theorem (section 2.7). Also the Argand loops are rather poorly correlated with the resonances (Collins, Ross and Squires (1969), Ringland and Phillips (1969); fig. 7.6) and the amplitude does not attain the smooth Regge asymptotic behaviour unless $\mathrm{Im}\{\alpha\}$ grows very rapidly with s, in which case the resonances become so wide as to disappear.

Although there have been many more sophisticated attempts to insert resonances with non-zero widths into the Veneziano formula none has proved very satisfactory because the constraints of analyticity and Regge asymptotic behaviour in all directions in the complex s plane are so restrictive (see for example Bali, Coon and Dash (1969), Cohen-Tannoudji *et al.* (1971)). To use it phenomenologically it is therefore necessary to employ the asymptotic form (7.4.8) despite the fact that it is invalid on the real positive s axis. Also, for phenomenology it is essential to be able to include higher-spin external particles, especially spin $= \frac{1}{2}$. This has been done (see Neveu and Schwarz 1971) but in order to satisfy the MacDowell symmetry these models contain parity doublets. Also, because the daughter sequences of the Veneziano model do not correspond to Toller pole sequences, infinite sums of Veneziano terms are needed to satisfy the conspiracy relations (6.5.7). We shall touch on some of these generalizations of the Veneziano model in chapter 9.

It is also important to note that (7.4.4) is certainly not unique. In fact the amplitude

$$A(s,t) = \sum_{l,m,n\geqslant 0} C_{lmn} V_{lmn}(s,t), \quad n \leqslant l+m \tag{7.4.14}$$

$$V_{lmn}(s,t) \equiv g\,\frac{\Gamma(l-\alpha(s))\,\Gamma(m-\alpha(t))}{\Gamma(n-\alpha(s)-\alpha(t))} \tag{7.4.15}$$

where C_{lmn} are arbitrary coefficients, also satisfies all the FESR and duality requirements. The V_{lmn} are known as Veneziano 'satellite' terms. They differ from (7.4.4) in having their first pole in s at $\alpha(s) = l$, and the asymptotic behaviour $s^{\alpha(t)+n-l}$, etc. Clearly $l = 0$ is possible only if the trajectory cuts $\alpha(s) = 0$ for $s > 0$, unlike fig. 7.5. This arbitrariness demonstrates the weakness of the FESR consistency conditions compared with the full bootstrap requirements which depend on unitarity.

Despite these problems, which have greatly limited its phenomenological application, the Veneziano model is a very useful theoretical 'toy', which, as we shall find in chapter 9, can readily be extended to multi-particle processes.

So far the model is suitable only for $\pi^+\pi^- \to \pi^+\pi^-$ which has exotic $I_u = 2$. If we assume that the f′ is decoupled from $\pi\pi$ (see section 5.2) the full amplitude will also have just the ρ–f exchange-degenerate trajectory as its leading trajectory (once the P component has been subtracted), but it is necessary to impose the isospin crossing relations (6.7.10), and the Bose statistics requirement that an amplitude of even isospin is even under the spatial parity transformation $z \to -z$, and vice versa. Thus the t-channel isospin amplitudes $A_t^I(s,t)$ might be written

$$\left.\begin{aligned} A_t^0(s,t) &= a(V(s,t)+V(t,u)) + bV(s,u) \quad \text{even under } s\leftrightarrow u \\ A_t^1(s,t) &= c(V(s,t)-V(t,u)) \quad \text{odd under } s\leftrightarrow u \\ A_t^2(s,t) &= V(s,u) \quad \text{even } s\leftrightarrow u, \text{ exotic } t \end{aligned}\right\} \tag{7.4.16}$$

(where a, b and c are constants), provided $V(s,t)$ is symmetric under $s\leftrightarrow t$, etc. Then applying the crossing relation (6.7.10)

$$A_s^I = \sum_{I_t} M(I_s, I_t)\, A_t^I$$

to (7.4.16) with the $\pi\pi$ crossing matrix of table 6.3, we find that to ensure that there are no poles in the exotic A_s^2 amplitude, i.e. to eliminate from it $V(s,t)$ and $V(s,u)$ terms, we need $a = \frac{3}{2}c$, and $b = -\frac{1}{2}$,

https://doi.org/10.1017/9781009403269.008 Published online by Cambridge University Press

while to make A_s^0 symmetric under $t \leftrightarrow u$ demands $c = 1$, so

$$\left.\begin{aligned} A_0^s(s,t) &= \tfrac{3}{2}(V(s,t)+V(t,u))-\tfrac{1}{2}V(s,u) \\ A_t^1(s,t) &= V(s,t)-V(t,u) \\ A_t^2(s,t) &= V(s,u) \end{aligned}\right\} \tag{7.4.17}$$

(Lovelace 1968). The residues of the t-channel poles in (7.4.17) in the three isospin states $I_t = (0,1,2)$ are obviously in the ratio $3:2:0$ which gives an eigenvector of the $\pi\pi$ crossing matrix with eigenvalue 1, i.e.

$$\begin{pmatrix} \frac{1}{3} & 1 & \frac{5}{3} \\ \frac{1}{3} & \frac{1}{2} & -\frac{5}{6} \\ \frac{1}{3} & -\frac{1}{2} & \frac{1}{6} \end{pmatrix} \begin{pmatrix} 3 \\ 2 \\ 0 \end{pmatrix} = \begin{pmatrix} 3 \\ 2 \\ 0 \end{pmatrix} \tag{7.4.18}$$

As $s \to \infty$ ($u \to -\infty$) at fixed t (7.4.7) in (7.4.17) gives

$$A_t^1 \xrightarrow[s\to\infty]{} \frac{g\pi(\alpha' s)^{\alpha(t)}}{\Gamma(\alpha(t))\sin\pi\alpha(t)}\left[e^{-i\pi\alpha(t)}-1\right] \tag{7.4.19}$$

the -1 coming from the $V(t,u)$ term. The square bracket in (7.4.19) is, of course, just the signature factor expected for the odd-signature $I_t = 1$ ρ pole. Similarly for A_t^0, which is even under $s \leftrightarrow u$, the terms $V(s,t)+V(t,u) \sim (e^{-i\pi\alpha(t)}+1)\,s^{\alpha(t)}$ for the even-signature f. We need to be careful about $V(s,u)$ however. This contains no poles in t, and hence should not contribute to the asymptotic behaviour in this limit. Now from (7.4.6) we find that

$$V(s,u) \sim e^{-cs}), \quad s \to \infty, \quad t \text{ fixed} \tag{7.4.20}$$

where c is a constant, provided that $\alpha_s' = \alpha_u'$, i.e. the slopes of the trajectories in the s and u channels are the same. For the crossing-symmetric $\pi\pi$ amplitude clearly this will always be true.

Now $V(s,t)$ in (7.4.7) vanishes when

$$\alpha(s)+\alpha(t) = 1, \quad \text{i.e. } 2\alpha^0+\alpha' s+\alpha' t = 1 \tag{7.4.21}$$

This zero will coincide with the Adler zero required by current algebra theory (see for example Renner (1968), Adler and Dashen (1968)) which makes the $\pi\pi$ amplitude vanish at the unphysical point $s = t = u = m_\pi^2$, if

$$\alpha^0 = \tfrac{1}{2} - \alpha' m_\pi^2 \tag{7.4.22}$$

(Weinberg 1966), and since the trajectory must reach $\alpha = 1$ for $t = m_\rho^2$ we have

$$\alpha' = \frac{1}{2(m_\rho^2 - m_\pi^2)} \approx 0.88\,\text{GeV}^{-2}, \quad \alpha^0 = 0.48 \tag{7.4.23}$$

in quite good agreement with (5.3.1) and figs. 5.5 and 6.6. Using these parameters for the trajectory good agreement is found between (7.4.4) and current algebra requirements (see Lovelace 1968) so despite its obvious defects the Veneziano model has many surprising and desirable properties for $\pi\pi$ scattering.

7.5 Duality and SU(3)

The construction of the $\pi\pi$ model (7.4.17) depends on the fact that once the P has been eliminated there is only a single leading trajectory in all the channels of $\pi\pi$ scattering, i.e. the isospin-degenerate ρ–f trajectory (since we assumed that the f′ does not couple to $\pi\pi$). It is thus convenient to refer to $V(s,t)$ in (7.4.17) as $V_{\rho\rho}(s,t)$ since ρ (and f) poles occur in both s and t. Exchange degeneracy was necessary because, using an obvious notation for the factorizable exchange couplings,

$$\left.\begin{aligned}\mathrm{Im}\{A(\pi^+\pi^-)\} &= (\mathrm{f}_{\pi\pi})^2+(\rho_{\pi\pi})^2\\ \mathrm{Im}\{A(\pi^+\pi^+)\} &= (\mathrm{f}_{\pi\pi})^2-(\rho_{\pi\pi})^2\end{aligned}\right\} \tag{7.5.1}$$

and strong exchange degeneracy gives

$$(\mathrm{f}_{\pi\pi})^2 = (\rho_{\pi\pi})^2 \tag{7.5.2}$$

and eliminates poles from the exotic $I=2$, π^+–π^+ amplitude.

If we now consider Kπ scattering, related to $\pi\pi$ by SU(3), there will be the same ρ–f trajectory in the t channel, $\pi\pi\to\mathrm{K}\bar{\mathrm{K}}$, but the exchange-degenerate K*–K** trajectory appears in both the s and u channels. To achieve the required symmetry we thus write

$$\left.\begin{aligned}A_t^0 &= a(V_{\rho\mathrm{K}^*}(t,s)+V_{\rho\mathrm{K}^*}(t,u)) \quad \text{even } s\leftrightarrow u\\ A_t^1 &= b(V_{\rho\mathrm{K}^*}(t,s)-V_{\rho\mathrm{K}^*}(t,u)) \quad \text{odd } s\leftrightarrow u\end{aligned}\right\} \tag{7.5.3}$$

the V_{ij} being like (7.4.4) but with different trajectories in the two channels ($I_t=2$ is not possible for $\mathrm{K}\bar{\mathrm{K}}$). However, in view of (7.4.20) we require $\alpha'_\rho=\alpha'_{\mathrm{K}^*}$, so only the intercepts of the trajectories can be different. To obtain the s-channel isospin amplitudes we use the πK crossing matrix of table 6.3 in the crossing relation (6.7.10), and to eliminate poles in the exotic $I_s=\frac{3}{2}$ state we need $a=(\sqrt{\frac{3}{2}})b$. This gives

$$\left.\begin{aligned}\mathrm{Im}\{A(\mathrm{K}^+\pi^+)\} &= \mathrm{f}_{\mathrm{K}\mathrm{K}}\mathrm{f}_{\pi\pi}-\rho_{\mathrm{K}\mathrm{K}}\rho_{\pi\pi}\\ \mathrm{Im}\{A(\mathrm{K}^+\pi^0)\} &= \mathrm{f}_{\mathrm{K}\mathrm{K}}\mathrm{f}_{\pi\pi}+\rho_{\mathrm{K}\mathrm{K}}\rho_{\pi\pi}\end{aligned}\right\} \tag{7.5.4}$$

and $\mathrm{f}_{\mathrm{K}\mathrm{K}}\mathrm{f}_{\pi\pi}=\rho_{\mathrm{K}\mathrm{K}}\rho_{\pi\pi}$, which together with our solution to (7.5.2) requires

$$\mathrm{f}_{\mathrm{K}\mathrm{K}}=\rho_{\mathrm{K}\mathrm{K}} \tag{7.5.5}$$

https://doi.org/10.1017/9781009403269.008 Published online by Cambridge University Press

Then KK and $K\bar{K}$ elastic scattering are similar, except that the $I = 0$ f and ω exchanges and the $I = 1$ ρ and A_2 exchanges all occur. So we can write

$$\left.\begin{aligned}
\mathrm{Im}\{A(K^+K^-)\} &= (f_{KK})^2 + (A_{2KK})^2 + (\omega_{KK})^2 + (\rho_{KK})^2 \\
\mathrm{Im}\{A(K^+K^+)\} &= (f_{KK})^2 + (A_{2KK})^2 - (\omega_{KK})^2 - (\rho_{KK})^2 \\
\mathrm{Im}\{A(K^+K^0)\} &= (f_{KK})^2 - (A_{2KK})^2 - (\omega_{KK})^2 + (\rho_{KK})^2 \\
\mathrm{Im}\{A(K^+\bar{K}^0)\} &= (f_{KK})^2 - (A_{2KK})^2 + (\omega_{KK})^2 - (\rho_{KK})^2
\end{aligned}\right\} \qquad (7.5.6)$$

the sign changes being those demanded by the signature and charge-conjugation properties of the exchanges. Since both K^+K^+ and K^+K^0 are exotic ($S = 2$) we require

$$(f_{KK})^2 = (\omega_{KK})^2 \quad \text{and} \quad (A_{2KK})^2 = (f_{KK})^2 \qquad (7.5.7)$$

with the ω and A_2 trajectories degenerate with f and ρ, which is indeed approximately true in fig. 5.4. However (7.5.7) and (7.5.3) imply

$$\rho_{KK} = \omega_{KK} \qquad (7.5.8)$$

while exact SU(3) for the couplings would give (see Gourdin 1967)

$$(\sqrt{3})\,\rho_{KK} = \omega_{KK} \qquad (7.5.9)$$

We can satisfy both these requirements by remembering that with broken SU(3) the physical ω particle may be a mixture of octet and singlet states (see (5.2.17)), and then the SU(3) symmetry requirement for the couplings becomes

$$(\sqrt{3})\,\rho_{KK} = \omega_{8KK} \qquad (7.5.10)$$

so if we take the ideal mixing angle given by (5.2.18), $\cos\theta = 3^{-\frac{1}{2}}$, both (7.5.8) and (7.5.10) will be satisfied. This means that the exchange-degenerate $\phi + f'$ trajectory will also be exchanged in KK scattering (but not in $\pi\pi$). And this is very desirable since (7.5.7) and (7.5.5) imply that $\mathrm{Im}\{A(K^+\bar{K}^0)\}$ in (7.5.6) vanishes; that is to say without a $\phi + f'$ contribution there would be no resonances in the $K^+\bar{K}^0$ channel despite the fact that it is not exotic.

All these relations can readily be described if the various particles are represented by their quark content, shown in table 5.2 (Harari 1969, Rosner 1969). All the incoming and outgoing mesons can be represented as $q_i\bar{q}_j$ where q_i, q_j = p, n or λ quarks. The condition we have been imposing on (7.5.1), (7.5.4) and (7.6.5) is that there should be no exotic resonances, so all the internal particles must also have the quantum numbers of the $\{1\} \oplus \{8\}$ representations of SU(3) which

https://doi.org/10.1017/9781009403269.008 Published online by Cambridge University Press

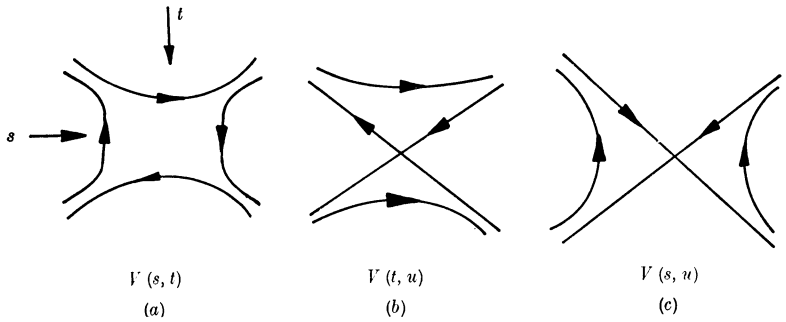

FIG. 7.7 Quark duality diagrams for meson–meson scattering. The arrow represents the direction of the quark; an anti-quark travels in the opposite direction to the arrow.

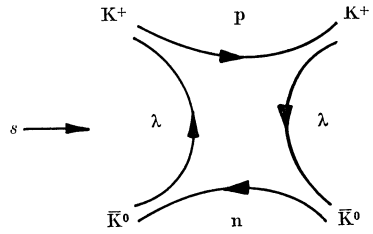

FIG. 7.8 The duality diagram for $K^+\bar{K}^0$ elastic scattering.

are also contained in $q\bar{q}$ (see (5.2.16)). So the duality diagram fig. 7.7 (a) can represent $V(s,t)$ for all our PS–PS meson scattering solutions, since it ensures quantum number conservation and only non-exotic $q\bar{q}$ states in both the s and t channels. However, the lines must not cross over each other as in fig. 7.7 (b), (c) or there would be exotics in one of the channels. But these crossed diagrams are suitable for the $V(s,u)$ and $V(t,u)$ terms respectively. Fig. 7.7 also incorporates our mixing-angle result (7.5.10) since in $K^+\bar{K}^0$ elastic scattering (fig. 7.8) only $\lambda\bar{\lambda}$, and hence with ideal mixing (equation (5.2.19)) only ϕ–f′, can be exchanged in the t channel. The ρ, f, ω and A_2 trajectories do not contribute to this process.

With exact SU(3) symmetry, meson–meson scattering is $\{8\} \otimes \{8\}$ scattering with amplitudes A_t^μ, $\mu = \{1\}, \{8_{ss}\}, \{8_{sa}\}, \{8_{as}\}, \{8_{aa}\}, \{10\}, \{1\bar{0}\}, \{27\}$ (see section 6.7). However, since $\{10\}$, $\{1\bar{0}\}$ and $\{27\}$ are exotic we need a solution which is an eigenvector of the $\{8\} \oplus \{8\}$ crossing matrix (table 6.4) having eigenvalue 1, and no trajectories in $\{10\}$, $\{1\bar{0}\}$ or $\{27\}$ (cf. (7.4.18) for isospin). Because of charge conjugation only symmetric d-type couplings are possible for the tensor $\{8\}$, and only anti-symmetric f-type couplings for the vector $\{8\}$. The

https://doi.org/10.1017/9781009403269.008 Published online by Cambridge University Press

eigenvector which satisfies these requirements is

$$A^{\mu} = (16, 5, 0, 0, 9, 0, 0, 0) \qquad (7.5.11)$$

which gives the coupling ratios for the singlet and octet trajectories.

These results can readily be extended to other meson scattering processes (Chiu and Finkelstein 1968) such as PS–V or V–V scattering. For the natural-parity exchanges the requirements are identical to the above, but in addition unnatural-parity exchanges can occur, and it is found necessary for the natural-C_n PS nonet (π, K, η, η') to be degenerate with the natural-C_n A^- nonet (B, Q, H?) and for the unnatural-C_n A^+ nonet (A_1, Q, D?) to be exchange degenerate with some axial tensor nonet. For each nonet the symmetry-breaking pattern should be similar to the natural-parity case. Quite apart from the fact that many of the required states have not been identified, we know that the η–η' mixing, for example, is far from ideal, so it would seem that in practice these duality constraints hold only for the leading natural-parity meson trajectories.

The duality diagrams also suggest how the internal symmetry requirements of duality can be satisfied in meson–baryon scattering, since we can represent all the external and internal baryons as $q_i q_j q_k$, i, j, k = p, n or λ quarks, as in fig. 7.9. This ensures that only non-exotic baryons occur in the s channel, and non-exotic mesons in the t channel. The corresponding su diagram has baryons in both channels.

When the SU(3) symmetry is broken, the exchange-degeneracy requirements on the meson exchanges in the $V(s,t)$ and $V(t,u)$ terms in PS–B scatterings are identical to those for PS–PS scattering (see Mandula *et al.* 1969). In fact we have already noted in table 7.1 (p. 220) the exchange-degeneracy requirements for ρ, ω, A_2 and f to prevent exotics in K^+p and pp, which are the same as those for $K^+\pi^+$ and $\pi^+\pi^+$.

Constraints on the baryon spectrum arise from the $V(s,u)$ term which controls backward scattering. The most plausible full solution (see Mandula, Weyers and Zweig 1970) requires the $J^P = \frac{1}{2}^+$ octet to be exchange degenerate with the $\frac{3}{2}^+$ decuplet, $\frac{3}{2}^-$ octet and $\frac{3}{2}^-$ singlet. But evidently this constraint is badly violated since, for example, the Δ trajectory is well separated from that of the N (see figs. 5.6), though the hyperon Λ and Σ trajectories seem to satisfy the constraint quite well (fig. 7.10). A Veneziano model for meson–baryon scattering can be constructed, using $V(s,t)$ etc., like (7.4.4) for the invariant A' and B amplitudes (equation (4.3.11)), with $\alpha \to \alpha - \frac{1}{2}$ for channels containing baryons (see for example White (1971)). A rather thorough discussion

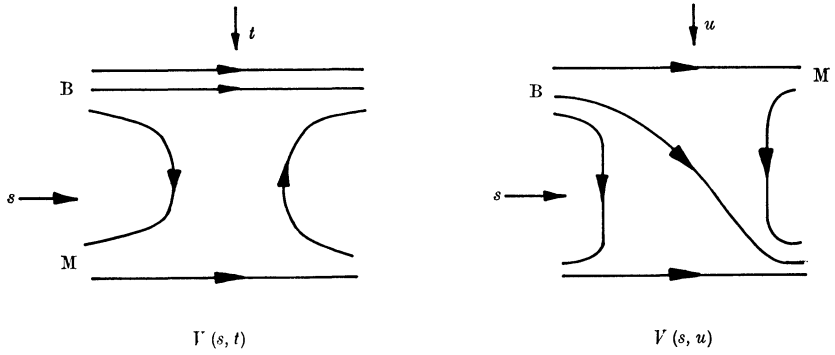

FIG. 7.9 Duality diagrams for meson–baryon scattering.

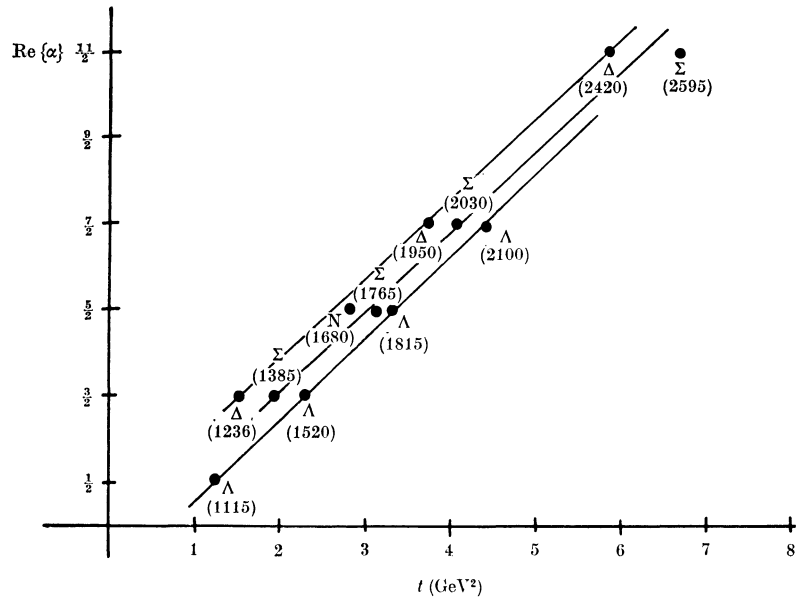

FIG. 7.10 Some examples of exchange-degenerate baryon trajectories. The splitting is much greater in most cases.

of the self-consistent, factorizing solutions for these cases has been given by Rimpault and Salin (1970). It seems probable, however, that to impose factorization constraints is too restrictive since, as we shall discuss below, phenomenologically duality seems to involve sums of cuts and poles rather than just poles.

When we come to examine baryon–anti-baryon scattering there are serious troubles because, for example, in $\Delta\Delta$ scattering $I = 0, 1, 2, 3$

https://doi.org/10.1017/9781009403269.008 Published online by Cambridge University Press

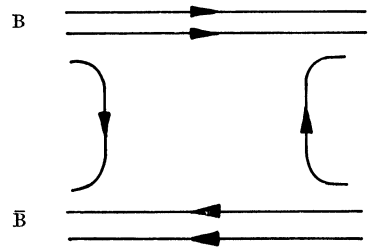

FIG. 7.11 Duality diagram for baryon–anti-baryon scattering.

are all possible, but to impose the absence of exotic mesons in $I = 2, 3$ in both the s and t channels requires that all the isospin amplitudes vanish (Rosner 1968). This is in fact rather obvious from the duality diagram in fig. 7.11 which must have a $q\bar{q}q\bar{q}$ intermediate state, and hence exotics. Thus either one must admit that duality fails for these higher-threshold channels, or conclude that exotic mesons exist which do not couple strongly to meson–meson scattering.

To summarize, the rules for drawing 'legal' duality diagrams are that in the limit of SU(3) symmetry we draw $\longrightarrow$ for a quark, and $\longleftarrow$ for an anti-quark, so each meson is represented by $\rightleftarrows$, and each baryon by $\equiv$. For a $B = 0$ channel we must be able to cut the diagram into two by just a $q\bar{q}$ state (not $q\bar{q}q\bar{q}$, etc.), and for a $B = 1$ channel by just a qqq state, so that there are no exotics. No quark lines may cross, i.e. we must have planar diagrams for each Veneziano term, and the two ends of each line must belong to different particles to preserve the ideal mixing (see Rosner 1969). This works for meson–meson and meson–baryon scattering but not for baryon–baryon scattering. We shall describe in section 9.4 how these rules can be extended to multi-particle processes.

7.6 Phenomenological implications of duality

There are many important consequences of the duality hypothesis which seem to be borne out experimentally. These include the pole dominance of the non-Pomeron part of scattering amplitudes, the absence of exotic resonances (which may help to explain why the quark model works), strong exchange degeneracy and nonsense decoupling, ideal mixing of SU(3) representations, the occurrence of parallel linear trajectories, and the fact that $s_0 = \alpha'^{-1}$. But we have also found that when pressed too hard the self-consistency of the

https://doi.org/10.1017/9781009403269.008 Published online by Cambridge University Press

duality scheme breaks down, so it is important to try and discover from experiment the extent to which these duality ideas hold good.

We have noted that although exchange degeneracy and ideal mixing seem to be valid for the vector and tensor mesons this is not the case for other exchanges. However, as these are the dominant exchanges in forward meson–baryon and baryon–baryon scattering, the duality rules work quite well for such processes. For example fig. 6.4 shows that the total cross-sections for exotic pp and K^+p are much flatter than those for $\bar{p}p$ and K^-p, and it seems very plausible that $\mathrm{Im}\{A^{\mathrm{el}}(K^+p)\}$ contains just the P, as required by two-component duality. But $\sigma^{\mathrm{tot}}(pp)$ does fall at low s, which indicates that the cancellation between the ω and f exchanges is not perfect in this case. These trajectories do of course contribute to $\mathrm{Re}\{A^{\mathrm{el}}\}$ (see (6.8.22)). The dips in $d\sigma/dt$ at $|t| \approx 0.55\,\mathrm{GeV}^2$, observed in medium energy $\bar{p}p$ and K^-p elastic scattering, and due to the nonsense zero of the R contribution, are conspicuously absent in pp and K^+p (fig. 6.5). This is a direct verification of the importance of s-channel quantum numbers in controlling the t-channel exchanges, and hence of duality.

Detailed fits of meson–baryon scattering using the Veneziano model for the R term have been attempted. It is first necessary to 'smooth' the amplitude by taking its asymptotic form (7.4.8) even for real positive s. To cope with the baryon spin it has been usual to use the Veneziano model for the invariant amplitudes $A'(s,t)$ and $B(s,t)$ introduced in (4.3.11) rather than helicity amplitudes, because the former have more simple crossing properties. The chief difficulties are that, since no cuts are included, baryon parity doublets automatically appear (see (6.5.13)), the scale factor has to be altered from α'^{-1} to obtain the observed exponential fall of $d\sigma/dt$ with t (note that g in (7.4.4) is a constant), satellite terms have to be introduced, and there is the cross-over zero problem of section 6.8*l* (see Berger and Fox 1969). So quantitative fits of the data with the Veneziano model are not really possible.

Another interesting consequence of duality (Barger and Cline 1970) is that since with ideal mixing the ϕ is made of $\lambda\bar{\lambda}$ quarks only, it is impossible to exchange a $q\bar{q}$ pair in the quasi-elastic process $\gamma p \to \phi p$, so P alone should be exchanged (fig. 7.12). The very flat energy dependence of this process even at low energies (fig. 7.13) suggests that this is indeed the case.

For inelastic processes, where P cannot contribute, strong exchange degeneracy requires the sort of line-reversal equalities whose (modest)

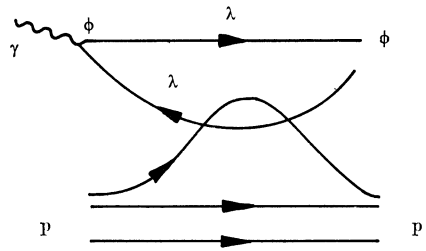

FIG. 7.12 A representation of P exchange in $\gamma p \to \phi p$. As the λ quarks are not exchanged down the diagram this has vaccuum quantum numbers but not $q\bar{q}$ in the t channel.

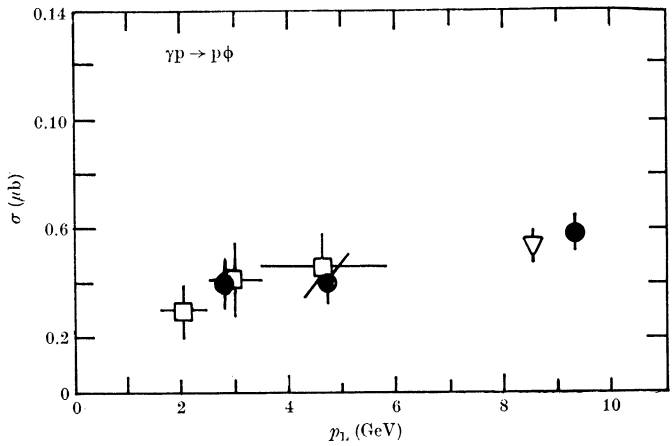

FIG. 7.13 Plot of $\sigma(\gamma p \to \phi p)$ versus laboratory momentum p_L, from Leith (1973).

success was described in section 6.8*h*. In particular $\mathrm{Im}\{A(s,t)\}$ should vanish identically for inelastic processes with exotic s-channel quantum numbers. Examples are $K^+n \to K^0p$ and $Kp \to K\Delta$ for which duality diagrams with $q\bar{q}$ meson exchanges cannot be drawn (fig. 7.14). More interesting are processes like

$$K^-p \to \pi^-\Sigma^+, \quad K^-n \to \pi^-\Lambda, \quad K^-n \to \pi^-\Sigma^0,$$

which are not exotic but for which no legal duality diagram can be drawn, so there must be a cancellation between K** and K* exchanges in $\mathrm{Im}\{A\}$. This also means that the resonances which occur in these processes must couple with alternating signs so that $\langle A^r \rangle \approx 0$ when averaged over a few resonances.

Similarly if the t channel is exotic, as in $\pi^-p \to \pi^+\Delta^-$ or $K^-p \to \pi^+\Sigma^-$,

https://doi.org/10.1017/9781009403269.008 Published online by Cambridge University Press

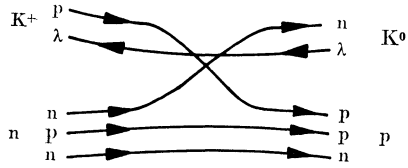

FIG. 7.14 Illegal duality diagram for $K^+n \to K^0p$.

since there are no t-channel exchanges, we must expect the resonances to cancel on average. This seems to work approximately for the former process but not the latter (Kernan and Sheppard 1969, Ferro-Luzzi *et al.* 1971). Duality diagrams make the further prediction that since $\phi = \lambda\bar{\lambda}$ it must decouple from inelastic (non-P exchange) processes involving only non-strange quarks. So processes like $\pi^-p \to \phi n$, $\pi^+p \to \phi\Delta^{++}$ should not occur. Their cross-sections certainly seem to be very small compared with similar allowed processes such as $\pi^-p \to \omega n$, $\pi^+p \to \omega\Delta^{++}$.

In general one concludes that the duality, exchange-degeneracy and ideal mixing requirements are moderately well satisfied for V and T exchanges, but certainly not exactly. But for most other exchanges, such as PS, $A^{\pm}$, or baryon, they are rather badly broken.

We have noted that strong exchange degeneracy demands nonsense decoupling, but found in section 6.8*k* that the choosing-nonsense hypothesis does not seem to be compatible with factorization, even for V and T exchanges. In fact it seems likely that pole–cut cancellation is needed to account for the dip in $d\sigma/dt(\pi N)$ near $\alpha = 0$ (see section 8.7*c* below). Similarly we have provisionally blamed the cross-over zero in $\mathrm{Im}\{A_{++}\}$ at $|t| \approx 0.15\,\mathrm{GeV}^2$ on pole–cut cancellation (section 6.8*l*). However, as we mentioned in section 7.3, both of these features are present in the low energy resonance contribution and it therefore seems as though duality works somewhat better than does the hypothesis that Regge pole exchanges dominate, and it might be better to write

$$\langle A^{\mathrm{r}} \rangle \approx A^{\mathrm{R}} + A^{\mathrm{c}} \qquad (7.6.1)$$

where A^{c} is the Regge cut amplitude, rather than (7.3.2).

Further evidence for this comes from π exchange processes like $\gamma p \to \pi^+ n$, $\pi p \to \rho p$, etc., where the resonances produce forward peaks which were explained in section 6.8*j* (see also section 8.7*f* below) as due to interference between the π pole and a self-conspiring cut, π_{c}. So we have $\langle A^{\mathrm{r}} \rangle \approx \pi + \pi_{\mathrm{c}}$. The Veneziano model can only account for such processes by including conspiring trajectories (Armad,

https://doi.org/10.1017/9781009403269.008 Published online by Cambridge University Press

Fayyazuddin and Riazuddin 1969) but such conspiracies are unsatisfactory (section 6.8*j*). Thus the pole-dominant solutions to the duality constraints can only be a rough approximation.

A further problem for the Veneziano model is that by no means all the required resonances have been observed. The leading ρ, ω, K* trajectories certainly seem to rise linearly to the $J = 3$ or 4 level, and baryon states up to perhaps $J = \frac{19}{2}$ are known, with no indication that higher-spin resonances may not be found eventually. But the daughter trajectories are much less well established. This may be partly because partial-wave analysis of the non-peripheral partial waves (i.e. $J < (\sqrt{s})\,R$, see section 2.2) is difficult because of contamination by the higher waves. However, there is no evidence for a ρ′(1275) daughter of the ρ, degenerate with the f (see fig. 7.5), and in fact strong evidence that it does not appear in the ππ channel. There is evidence of a heavier broad ρ′(1600), which couples more to 4π than 2π (see Particle Data Group 1974). This could be the daughter of the g(1680), which suggests that perhaps only the odd daughters of the ρ trajectory occur.

Many more baryon resonances are known, but fig. 5.6 shows that it is not a simple matter to fit them into daughter sequences. In any case high-mass, low-spin resonances are expected to be wide because of the large number of decay channels available to them, so the narrow resonance approximation will probably be poor at the daughter level, and it seems more plausible to regard the daughter sequences of the Veneziano model as simply a δ-function approximation to the channel discontinuities. In the next chapter we shall show why absorption is expected to be much stronger for low partial waves than higher ones, and it seems likely that pole dominance works best for the peripheral partial waves, $J \approx (\sqrt{s})\,R$. Of course with linear trajectories there will be resonances in the super-peripheral partial waves up to $J_{\max} \approx \alpha' s$ so pole dominance may in fact be satisfactory for $\alpha' s \gtrsim J \gtrsim (\sqrt{s})\,R$, but in the Veneziano model the resonances with $J \gg (\sqrt{s})\,R$ have rather small widths, and those with $J \approx (\sqrt{s})\,R$ dominate (see fig. 7.15). (This must be so because the Veneziano model reproduces the observed peripheral forward peak.)

Despite these limitations the Veneziano model has had one additional and rather surprising success, in predicting amplitude zeros. The Γ-function in the denominator of (7.4.15) means that $V(s,t)$ has a zero along the line

$$\alpha(s) + \alpha(t) = p \qquad (7.6.2)$$

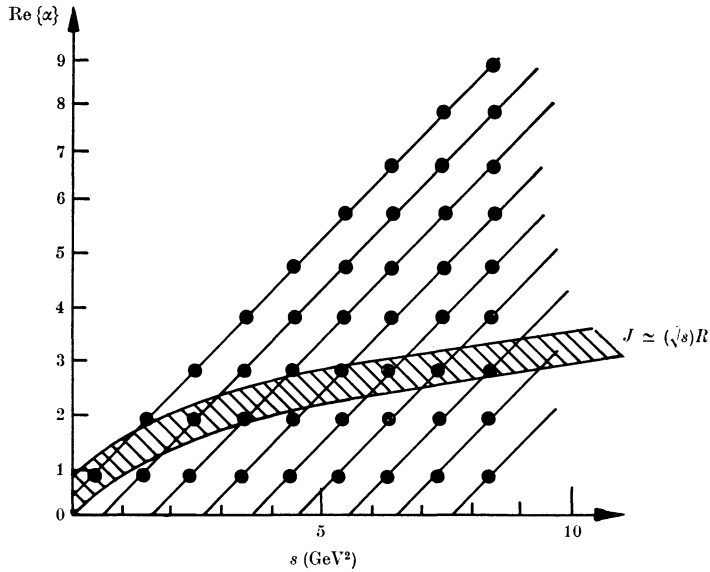

FIG. 7.15 The resonances of the Veneziano model and the peripheral region (shaded).

where p = an integer $\geqslant$ n. With parallel linear trajectories (7.6.2) implies

$$\alpha_s^0 + \alpha_t^0 + \alpha'(s+t) = p \tag{7.6.3}$$

or, from (1.7.21), $$u = \frac{\alpha_s^0 + \alpha_t^0 - p}{\alpha'} + \Sigma = \text{constant} \tag{7.6.4}$$

So zeros of the amplitude are predicted along lines of constant u.

The occurrence of these zeros in the unphysical region $s, t > 0$ is of course necessary to prevent double poles (see fig. 7.4), but the zeros are also predicted to continue into the physical region. Of course if the other terms $V(s,u)$, $V(t,u)$ are added these zeros may be removed, but in a process such as $K^- p \to \bar{K}^0 n$, for which the u channel is exotic so only $V(s,t)$ occurs, dips may be expected at fixed u, spaced by $\alpha'^{-1} \approx 1\,\text{GeV}^2$. These dips should occur despite the fact that there are no u-channel poles, because they stem from a cancellation between the s-channel Λ, Σ^0 poles and the t-channel ρ, ω, f, A_2 poles. Fixed zeros are in fact found at $u = -0.1$, -0.7 and $-1.7\,\text{GeV}^2$ (Odorico 1971). This is not exactly where the Veneziano model would predict them, but in view of its approximate nature some displacement is to be expected.

Odorico (1972) has shown that such fixed zeros are quite a general

https://doi.org/10.1017/9781009403269.008 Published online by Cambridge University Press

feature of scattering amplitudes. Since the addition of any sort of correction term will move a zero (unlike a pole) it is very remarkable that this feature of the Veneziano model should be observable, particularly in view of its various other deficiencies.

7.7 Conclusions

From the preceding discussion it will be evident that the status of the duality concept is still rather uncertain.

On the one hand it seems remarkable that it is possible even to construct a reasonably self-consistent model like (7.4.4) which satisfies so many of the duality requirements, and contains so many successful predictions. In fact when the model is made more 'physical' by including finite widths for the resonances, SU(3) breaking for the trajectory intercepts, and the P contribution is added, it bears quite a strong resemblance to the real world, and provides a plausible explanation for such facts as the absence of exotic resonances, ideal mixing, parallel linear exchange-degenerate trajectories, and $\alpha'^{-1} \approx s_0$. But unfortunately this physical model is not self-consistent because of the ancestor problem, the occurrence of exotics in $B\bar{B}$ channels, etc., and it does not agree quantitatively with experiment.

This could be because duality is only approximately valid. Alternatively, it might be an exact principle, all our difficulties stemming from the failure to incorporate unitarity, and especially Regge cuts, properly. But there do not seem to be any very compelling arguments in favour of duality as a basic law of strong interactions. All the very tight restrictions of dual models which give them predictive power come from the adoption of meromorphic scattering amplitudes (see for example Oehme 1970) (i.e. amplitudes containing only poles, no cuts), and once cuts are permitted it is not even clear how to formulate the duality idea.

One suggestion has been that one can regard the Veneziano model as a sort of 'Born approximation' for strong interactions, which should be iterated in the unitarity equations (as in section 3.5) to produce the physical S-matrix. In this case loop diagrams like fig. 1.11(b) will occur corresponding to the re-normalization of the masses, and couplings of the resonances. We shall examine some of these ideas briefly in chapters 9 and 11. So far they still seem to suffer from the usual ambiguities concerning the convergence of the Born series and double counting of terms, though such problems may eventually be overcome.

There is, however, one further very important feature of the Veneziano model which we shall look at in chapter 9. It is comparatively easy to generalize to many-particle scattering amplitudes, and provides a parameterization of the amplitudes which exhibits both resonance dominance at low energies and Regge asymptotic behaviour, with factorizable couplings for all the trajectories, in all the different channels. This has greatly facilitated the application of Regge theory to many particle processes. So, even if the duality idea should turn out not to be a fundamental principle of strong interaction dynamics, dual models will still have their uses, both as a mnemonic for many of the basic facts of two-body processes, and as a simplifying model for more complex ones.